



OpenFAST Modeling of the T-Omega Wind Floating Offshore Wind Turbine System

Preprint

Lu Wang,¹ Jason Jonkman,¹ Jim Papadopoulos,²
Andrew T. Myers^{2,3}

1 National Renewable Energy Laboratory

2 T-Omega Wind Inc.

3 Northeastern University

Presented at the ASME 2023 5th International Offshore Wind Technical Conference

Exeter, United Kingdom

December 18–19, 2023

**NREL is a national laboratory of the U.S. Department of Energy
Office of Energy Efficiency & Renewable Energy
Operated by the Alliance for Sustainable Energy, LLC**

This report is available at no cost from the National Renewable Energy Laboratory (NREL) at www.nrel.gov/publications.

Contract No. DE-AC36-08GO28308

Conference Paper
NREL/CP-5000-87168
January 2024



OpenFAST Modeling of the T-Omega Wind Floating Offshore Wind Turbine System

Preprint

Lu Wang,¹ Jason Jonkman,¹ Jim Papadopoulos,²
Andrew T. Myers^{2,3}

1 National Renewable Energy Laboratory

2 T-Omega Wind Inc.

3 Northeastern University

Suggested Citation

Wang, Lu, Jason Jonkman, Jim Papadopoulos, Andrew T. Myers. 2024. *OpenFAST Modeling of the T-Omega Wind Floating Offshore Wind Turbine System: Preprint*. Golden, CO: National Renewable Energy Laboratory. NREL/CP-5000-87168.
<https://www.nrel.gov/docs/fy24osti/87168.pdf>.

**NREL is a national laboratory of the U.S. Department of Energy
Office of Energy Efficiency & Renewable Energy
Operated by the Alliance for Sustainable Energy, LLC**

This report is available at no cost from the National Renewable Energy Laboratory (NREL) at www.nrel.gov/publications.

Contract No. DE-AC36-08GO28308

Conference Paper
NREL/CP-5000-87168
January 2024

National Renewable Energy Laboratory
15013 Denver West Parkway
Golden, CO 80401
303-275-3000 • www.nrel.gov

NOTICE

This work was authored in part by the National Renewable Energy Laboratory, operated by Alliance for Sustainable Energy, LLC, for the U.S. Department of Energy (DOE) under Contract No. DE-AC36-08GO28308. Funding provided by the U.S. Department of Energy Office of Energy Efficiency and Renewable Energy Wind Energy Technologies Office. The views expressed herein do not necessarily represent the views of the DOE or the U.S. Government. The U.S. Government retains and the publisher, by accepting the article for publication, acknowledges that the U.S. Government retains a nonexclusive, paid-up, irrevocable, worldwide license to publish or reproduce the published form of this work, or allow others to do so, for U.S. Government purposes.

This report is available at no cost from the National Renewable Energy Laboratory (NREL) at www.nrel.gov/publications.

U.S. Department of Energy (DOE) reports produced after 1991 and a growing number of pre-1991 documents are available free via www.OSTI.gov.

Cover Photos by Dennis Schroeder: (clockwise, left to right) NREL 51934, NREL 45897, NREL 42160, NREL 45891, NREL 48097, NREL 46526.

NREL prints on paper that contains recycled content.

OPENFAST MODELING OF THE T-OMEGA WIND FLOATING OFFSHORE WIND TURBINE SYSTEM

Lu Wang¹, Jason Jonkman¹, Jim Papadopoulos², Andrew T. Myers^{2,3}

¹National Renewable Energy Laboratory, Golden, CO

²T-Omega Wind Inc., Boston, MA

³Northeastern University, Boston, MA

ABSTRACT

To reduce the cost of offshore wind energy through a more efficient design of the floating support structure, T-Omega Wind developed a novel lightweight and shallow-draft platform concept that aims to achieve a wave-following behavior without resonance amplification. The rotor and generator are carried by four tower legs with each leg supported by a shallow-draft float at the base. In preparation for a more detailed analysis, a coupled aero-hydro-elastic model of the proposed concept is developed in OpenFAST. The detailed modeling approach is presented, including a novel application of the SubDyn substructure dynamics module of OpenFAST to approximate the loads on the axle tube at the tower top from the rotor hub bearings. Preliminary results obtained with the OpenFAST model by rigidifying the substructure and blades indicate that the original sizing of the design can lead to large hub acceleration in the axial/surge and pitch directions due to platform-pitch motion. The high axial acceleration also potentially leads to large bending moments in the four tower legs. To address these issues, an updated design is developed with, among other changes, increased float spacing at the tower base and improved shear-transmitting geometry of the tower legs. The new design suggests significantly reduced extreme hub accelerations under the same conditions even with structural flexibility and will be further analyzed in the future through full aero-hydro-servo-elastic simulations.

Keywords: FOWT; lightweight; shallow draft; hydroelasticity; OpenFAST

1. INTRODUCTION

Current designs of floating offshore wind turbine (FOWT) systems are often influenced by the platform designs from the oil and gas industry and make use of wind turbines similar to land-based wind turbines with limited motion tolerance. To minimize wave-excited motion, wave-transparent designs (which include semisubmersibles and spars) typically feature a relatively small waterplane area and a large displacement so that the resonance

frequencies of the platform motion are kept below energetic wave frequencies. However, the large underwater structure also results in the floating substructure accounting for close to 30% of the levelized cost of energy [1].

To further reduce the cost of offshore wind energy, T-Omega Wind (TOW) developed an unconventional platform and turbine configuration specifically for floating offshore wind energy applications. It is potentially more efficient structurally and supports easier production, installation, and maintenance. This design, initially proposed in Ref. [2] by TOW, consists of four widely spaced and shallow-draft floats arranged in a square. The floats support a four-legged tower structure that carries the wind turbine rotor and generator, with two legs upwind of the rotor and the other two downwind. In contrast to conventional designs that aim to minimize wave-excited motion, the TOW design intends to achieve a wave-following behavior, where each shallow-draft float of the platform moves up and down with the free water surface without resonance amplification to realize a lightweight and shallow-draft platform. The four-legged tower design is potentially more structurally efficient and supports the rotor and generator with less material. Note that the present wind-oriented four-legged tower arrangement with a tower-top axle tube is similar to the Eolink platform design [3, 4], but the present platform is lighter and is moved more by the waves. Furthermore, it also features a tension brace that directly connects the tower top to the mooring fairlead hinged to the platform to transmit the rotor thrust directly to the mooring line, bypassing the main support structure. The TOW design is expected to cut costs through lowered material use, a simpler mooring system, and reduced maintenance cost and downtime from easier disconnection and towing.

Preliminary analysis of the proposed concept for a 10-MW turbine is presented in Ref. [2]. The motion of the wind turbine was estimated for a range of sea states with significant wave heights up to 20 m based on the idealized assumption that the vertical motion of each float of the platform follows the wave elevation exactly, without delay or resonance amplification, while constrained by an infinitely stiff mooring line. Surge and

yaw motions of the turbine were estimated considering, respectively, the surge-heave coupling through the angled mooring line and the rotor gyroscopic effects including hydrodynamic yaw drag. With those kinematic assumptions, the peak vertical and horizontal turbine accelerations were found to remain below $0.5g$, where g is the gravitational acceleration, for all wave conditions. The blade root bending moment was also well below the allowed level found in the literature [2]. These results suggested the concept's feasibility and motivated exploration of those assumptions, see Ref. [5].

In Ref. [5], the platform's linear hydrodynamic behavior was explored in regular waves for various mass distributions. A simplified 2D potential-flow model of a rigid system was used with a linear-spring mooring line of high compliance. The desired wave-following behavior was mostly achieved under an ideal configuration where the floats are dynamically decoupled in heave via the mass distribution. However, when the center of gravity is raised or when the pitch moment of inertia is increased, the platform increasingly deviates from the ideal wave-following behavior and can potentially have a pitch resonance frequency coinciding with common wave frequencies.

To support more realistic modeling, we develop a coupled aero-hydro-elastic model of the TOW FOWT concept using the OpenFAST open-source modeling tool [6] for offshore wind turbines. This article provides a description of the modeling strategies along with preliminary simulation results (particularly, response amplitude operators [RAOs] of the pitch and heave motion of the rotor hub) for different platform configurations. The RAOs are used to estimate system responses in the frequency domain based on a publicly available 40-year environmental contour of the North Atlantic region to tune the overall geometry and sizes of major structural members.

2. OVERVIEW OF THE TOW FOWT CONCEPT

Figure 1 shows the overall arrangement of the TOW FOWT concept. A key feature of this design is the four shallow-draft floats. Each float has a cone-shaped bottom section and a cylindrical middle section. (A top cylindrical buoyancy unit shown in Figure 2, now abandoned, was originally used to tune the righting curve.) At equilibrium, the still water surface intersects the conical bottom section of each float. The cone shape is selected for its low added mass in heave, raising the heave natural frequency in pursuit of wave-following behavior. The apex angle of the cone is 105 deg following Ref. [5], resulting in an isolated-float heave RAO that increases monotonically with wavelength to unity without resonance amplification. For any wavelength of practical relevance, an isolated float will heave to follow the free surface with near-equal amplitude and zero phase shift. However, when four floats are joined to form a platform supporting a turbine, the platform might not be perfectly wave-following. Depending on the mass distribution, the pitch resonance frequency can potentially coincide with common wave frequencies if not carefully designed [5].

The four floats support a four-legged tower. The tower legs are joined together at the hub level by an axle tube. The rotor hub

spins about the axle tube as illustrated in Figure 3. The generator stator and rotor are placed between the wind turbine blades and the upwind legs. Compared to conventional designs with a single tower and a nacelle, the four-legged tower and the axle tube provide more efficient support to the direct-drive generator and wind turbine rotor. This helps in tolerating the increased hub and blade accelerations.

For the present analysis, the aeroelastic model of the 10-MW reference offshore wind turbine developed under the International Energy Agency (IEA) Wind Technology Collaboration Programme is used [7]. A key modification to the reference turbine design is the elimination of the rotor precone angle. Note that any prototype of the TOW design will require a custom-designed wind turbine with greater motion tolerance. The IEA Wind 10-MW reference wind turbine model is only included as a placeholder to conduct the hydroelastic platform analysis presented in this article.

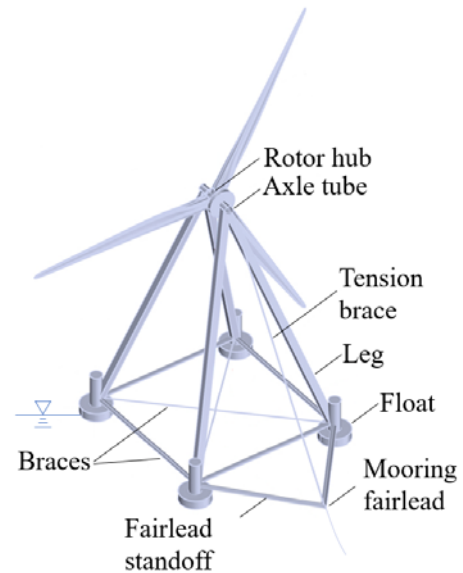


FIGURE 1: A LIGHTWEIGHT AND SHALLOW-DRAFT FLOATING OFFSHORE WIND TURBINE CONCEPT.

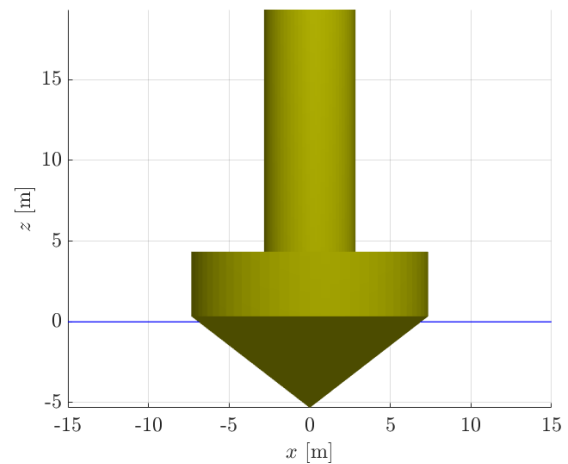


FIGURE 2: PROFILE OF A SINGLE FLOAT. THE HORIZONTAL LINE INDICATES THE STILL WATER LEVEL.

A single-line mooring is used to allow the whole platform to yaw freely to align with the incident wind direction, like a ship at anchor. This is necessary for the TOW concept due to the lack of a nacelle that can yaw independently from the rest of the support structure. It is recognized that achieving alignment in all wind and current conditions may require not only careful aerodynamic design, but also some actuated ability to impose corrective yaw moments.

To moor the FOWT, TOW envisions the use of a neutrally buoyant synthetic rope, optionally with subsurface floats and clumped weights for increased compliance and reduced heave-surge coupling [2]; however, the exact design of the mooring is not finalized and awaits completion of the global sizing exercise presented in this article. A tension brace connects the mooring fairlead and the axle tube at the hub level, and the fairlead standoff is hinged at the connections to the floats and can pitch freely about the sway axis. By design, the mooring line at the fairlead is approximately aligned with the tension brace. This arrangement is intended to allow the rotor thrust to be directly transmitted to the mooring system, thus minimizing platform pitch offset from wind thrust while reducing thrust-induced loads in the tower legs.

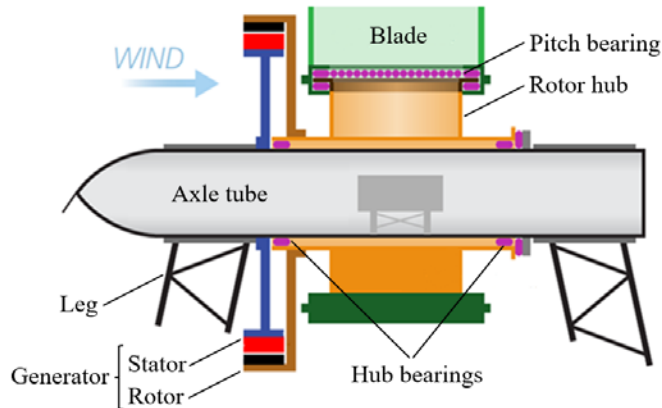


FIGURE 3: TOWER-TOP ASSEMBLY. NOTE THAT THE MOST UP-TO-DATE DESIGN USES TUBES INSTEAD OF LATTICE STRUCTURES FOR THE LEGS.

Selected dimensions and mass properties of the original design used in this analysis are summarized in Table 1 and Table 2. Key properties of the IEA Wind 10-MW reference offshore wind turbine can also be found in Ref. [7].

TABLE 1: SYSTEM DIMENSIONS

Dimension	Value	Unit
Float center-to-center distance	70.0	m
Hub height from still water level	120	m
Axle length between legs	12.3	m
Draft	5.30	m
Upwind distance from rotor to fairlead	98.2	m
Maximum float diameter	14.7	m
Float cone height	5.67	m

TABLE 2: MASSES OF KEY COMPONENTS

Component	Mass	Unit
Mass of floats	410	Metric ton
Mass of tower legs	155	Metric ton
Rotor mass (hub, blades, and generator rotor)	299	Metric ton
Axle assembly mass (axle tube, generator stator, generator add-on)	143	Metric ton
Structural bracing and mooring standoff	89	Metric ton
Total mass	1,095	Metric ton

3. OPENFAST MODELING

A coupled aero-hydro-elastic model of the TOW design is developed in the OpenFAST tool [6]. The hydroelastic modeling of the unconventional platform design necessitates the application of several new capabilities of OpenFAST recently developed for modeling substructure flexibility and member-level loads, as well as nonlinearities in the hydrodynamic and hydrostatic loads [8–10].

3.1 Modeling of structural dynamics

With conventional single-tower designs, typically the substructure dynamics is modeled using the SubDyn module [11] of OpenFAST, while the tower and blades are modeled using the ElastoDyn module of OpenFAST. The former solves a linear frame finite-element model of the substructure with Timoshenko beam theory and Craig-Bampton dynamic reduction. The latter solves the tower and blade bending using a modal representation with Euler-Bernoulli beam theory and consideration of some geometric nonlinearities. The mode shapes of the tower and blades used as inputs to ElastoDyn are determined with a finite-element preprocessor. The motion and load are matched between the SubDyn substructure model and the ElastoDyn tower model at an interface joint, typically at the tower base/transition piece. This modeling approach, however, cannot be applied to the TOW design with four inclined tower legs because ElastoDyn only supports a single vertical tower. An alternative approach is required.

To overcome the ElastoDyn limitation, we opt to model the entire support structure, including the four-legged tower, in SubDyn, as shown in Figure 4. Apart from the tension brace connecting the mooring fairlead and the axle tube, all flexible structural members are modeled using Timoshenko beam elements with bending, shear, axial, and torsional degrees of freedom (DoF). The tension brace is modeled as a cable element that behaves like a linear spring. Most joints are modeled as fixed joints, across which the 6-DoF motion of adjoining elements are transferred. One exception is the two joints connecting the mooring fairlead standoff to the floats, which are modeled as pin joints that pivot freely about the sway axis as discussed in Section 2. Other joint types are also utilized at the tower top (see Figure 5). The four floats are modeled as rigid; therefore, they are only represented as concentrated masses with moments of inertia in the structural model that are rigidly attached to the corresponding leg-base joints.

Craig-Bampton dynamic reduction is utilized to reduce the number of DoF of the finite-element model by only retaining the

six Guyan modes (also called interface or boundary modes) associated with the 6-DoF motion of the interface point between SubDyn and ElastoDyn and a predetermined number of low-frequency internal elastic Craig-Bampton modes (the Craig-Bampton mode shapes are obtained with the interface point fixed). Instead of solving for all DoF of the full finite-element model, SubDyn solves the equations of motion of only the retained Craig-Bampton modes, while ElastoDyn solves the equations of motion of the Guyan modes. The remaining high-frequency elastic modes are solved quasi-statically and superimposed onto the dynamic solution, based on the static-improvement method [11].

SubDyn was originally designed for fixed-bottom substructures but was recently upgraded to support floating substructures [8, 10]. This is primarily achieved through solving the Craig-Bampton and quasistatic modes in a moving/rotating frame of reference that follows the six Guyan interface modes, which, for a floating platform, correspond to the rigid-body motion of the platform following the motion of the interface point between SubDyn and ElastoDyn shown in Figure 4 and Figure 5. For the present model, the first 40 Craig-Bampton modes are retained in the dynamic solution, up to a natural frequency of 9.2 Hz. Note that this is the natural frequency of the substructure in isolation obtained with the interface point fixed and without external load and gravity. Therefore, it will differ from full system natural frequencies when floating in water. The rest of the substructure modes are solved quasi-statically.

With the tower legs also modeled in SubDyn, the interface point between SubDyn and ElastoDyn is moved up to the hub level (see Figure 5) instead of at the tower-base as would normally be the case for a conventional FOWT design. A very short and rigid dummy tower is prescribed in ElastoDyn with the “tower base” located at the interface point. This approach effectively allows us to model the tower in SubDyn instead of in ElastoDyn. Note that this approach can occasionally be helpful when modeling conventional single-tower designs as well because the SubDyn Timoshenko beam elements have additional shear, axial, and torsional DoF not modeled by ElastoDyn, and SubDyn does not require bending mode shapes to be precomputed as part of the inputs. However, one drawback of this approach is that the aerodynamic load on the tower and the tower-blockage and tower-shadow effects on the rotor cannot be modeled. OpenFAST presently only supports aerodynamic modeling of a single vertical tower, and the tower aerodynamic drag can only be mapped to the tower model in ElastoDyn. We are currently planning future software development within OpenFAST to support aerodynamic modeling of complex tower arrangements with aerodynamic load mapping to SubDyn to overcome this limitation. Another drawback is that the SubDyn substructure model is inherently linear, whereas ElastoDyn also models geometric nonlinearities in the tower. This simplification can potentially create difficulties with conventional single-tower designs when the tower deflection is large. However, this is possibly less critical with the present four-legged tower design that reduces tower-top deflection.

The axle tube at the tower top ties the top of the tower legs together. It also supports the generator and the wind turbine rotor. The preliminary analysis in Ref. [2] further suggests the tower-top pitch and yaw moments from the rotor potentially pose a design challenge. As a result, the loads along the axial tube and at the bearings are of significant interest. For this purpose, a novel application of SubDyn is utilized to estimate the loading in the axle tube and bearings. Details of the SubDyn model at the tower top are shown in Figure 5.

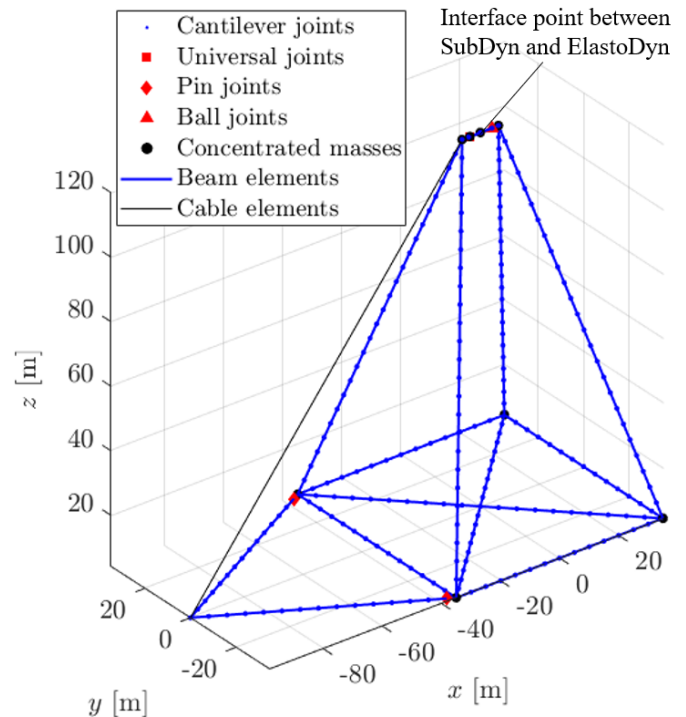


FIGURE 4: LINEAR-FRAME FINITE-ELEMENT MODEL OF THE PLATFORM SHOWN IN FIGURE 1 DEVELOPED WITHIN THE SUBDYN MODULE OF OPENFAST.

A Timoshenko beam connecting the upstream and downstream axial receivers (the joints between the axle tube and the tower legs) represents the axle tube. Along this axle beam, several point masses (with moments of inertia) are attached to represent the additional masses/inertias of the axle receivers, the generator stator, and generator add-on (additional generator components apart from the stator). Parallel and slightly offset from the axle tube, a second beam is included to represent the rotor hub, which, in actuality, is concentric with the axle tube. At the locations of the hub bearings (see Figure 3), two short beams representing the bearings attach the hub beam to the axle beam. It is not physical to represent the hub and the bearings as beams; therefore, we simply model them as effectively rigid with a much higher stiffness compared to the axle beam.

To approximate the load transfer through the hub bearings, the downwind beam representing the bearing is connected to the hub beam through a ball joint, which only transfers force but not moment. The beam representing the upwind bearing connects to the hub beam through a universal joint that transfers not only

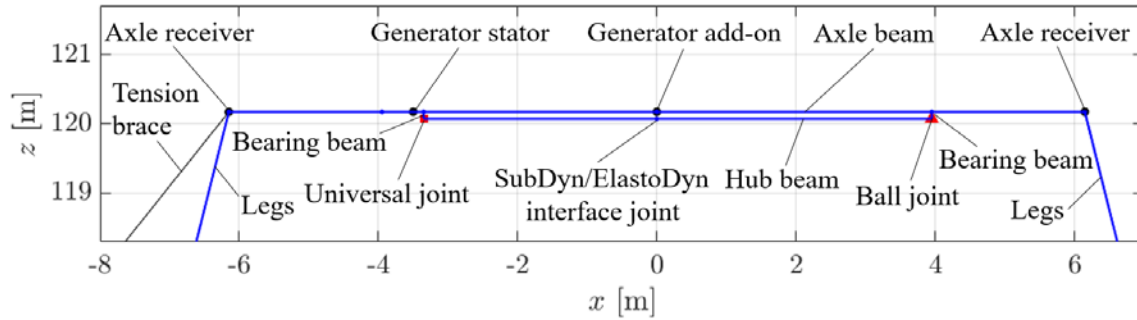


FIGURE 5: DETAILS OF THE SUBDYN MODEL AT THE HUB LEVEL REPRESENTING THE ASSEMBLY SHOWN IN FIGURE 3. SEE LEGEND OF FIGURE 4 FOR JOINT AND ELEMENT TYPES.

force but also the moment component along the hub axis to represent the moment transfer between the generator rotor and stator. The load from the wind turbine rotor from ElastoDyn is applied to the hub beam at the SubDyn/ElastoDyn interface joint. The exact point of load application is not critical because the hub beam is effectively rigid.

Note that this approach delivers only an approximate model of the axle tube and the rotor hub. One important simplification, apart from the rigid-beam representation of the hub and bearings, is that the hub beam in the SubDyn model is not actually spinning because that is not compatible with the linear structure assumption. The rigid-body motion of the generator is actually accounted for within the ElastoDyn module with the loads mapped to SubDyn. The SubDyn module of OpenFAST is not designed for detailed modeling of the wind turbine drivetrain. Nevertheless, we believe this approach can provide meaningful load estimates at least along the axle tube. A similar approach can potentially be used to approximate the loads in the drivetrain of conventional wind turbines as well using SubDyn [12].

Finally, the elasticity of the turbine blades is modeled in ElastoDyn using Euler-Bernoulli beam theory with predefined blade-bending mode shapes and neglecting blade torsion. The aeroelastic model of the IEA Wind 10-MW reference offshore wind turbine is adopted without modification apart from removing the precone [7].

3.2 Modeling of hydrodynamic loads

The hydrodynamic and hydrostatic loads on the four floats are modeled using the HydroDyn module of OpenFAST. The loads on the braces and the mooring fairlead standoff, should they become wetted, are neglected in the current modeling effort. This is because we intend to keep these members dry under most conditions with the final design.

The hydrodynamic loads on the floats are modeled using linear potential-flow wave radiation and wave diffraction theory, leveraging the ability to incorporate multiple potential-flow bodies within a single substructure recently added to HydroDyn [8, 10]. While full hydrodynamic coupling between the floats can be incorporated in HydroDyn, we opt to neglect it at this stage considering the large spacing between the floats relative to the float dimension. This simplification allows us to solve the frequency-domain wave excitation and wave radiation coefficients with a single float in isolation. This is convenient at

the present design stage because the potential-flow solution for each float does not need to be updated when exploring the effects of different choices of float spacing. Future modeling efforts with a more finalized design can incorporate hydrodynamic coupling among the floats together with second-order potential-flow sum- and difference-frequency wave excitation.

The wave radiation load on the floats is computed using the infinite-frequency added mass/moment of inertia, along with the time convolution of the float velocities with the radiation impulse-response functions that account for the free-surface memory effect [13]. The wave excitation is precomputed before the start of the time-domain simulation based on the wave spectrum using inverse discrete Fourier transform. However, instead of computing a single set of wave excitation time series for each float, multiple sets are precomputed with the structure centered at different points in a horizontal 2D grid. During the time-domain simulation, the wave excitation on the floats is then interpolated from the multiple sets of wave excitation time series based on the instantaneous position of the structure within the grid at each time step. This approach essentially corrects the phase of the wave excitation to account for the effects of any constant offset or drift motion of the platform in the wave direction [9]. This phase correction is critical to correctly capture the wave-following behavior in shorter waves.

In addition to the potential-flow hydrodynamic loads, strip-theory quadratic drag forces in the axial (heave) and transverse direction are also applied to the floats based on the relative velocity between the floats and the incident wave field. The added drag forces are evaluated up to the instantaneous free surface using vertical wave stretching.

For the preliminary analysis presented in this article, the hydrostatic load is evaluated using the linear hydrostatic stiffness matrix for simplicity. However, this approach can potentially result in large error due to the rapidly changing waterplane area with draft of the cone-shaped floats. For future analysis, nonlinear and exact hydrostatic load based on pressure integration over the instantaneous wetted surface can be used to check the impact of nonlinear hydrostatics. This is made possible by a new capability recently implemented in HydroDyn.

The components of hydrodynamic and hydrostatic force and moment on each float from HydroDyn are automatically mapped to the nearest structural node in the SubDyn model, which, in the

present setup, is the leg-base joint associated with each float. This load mapping enables a coupled hydroelastic simulation.

3.3 Modeling of the mooring system

To demonstrate the feasibility of eventually using a lumped-mass dynamic model for the taut mooring system, a preliminary model is developed within the MoorDyn module of OpenFAST. This model is illustrated in Figure 6. A subsurface float and a clumped weight are included to increase compliance and reduce the surge-heave coupling identified in Ref. [2]. This model is found to be numerically stable, demonstrating the feasibility of an unsteady mooring model coupled with the SubDyn substructure model in future numerical simulations.

However, for the present initial design effort in sizing the platform, a simple linear-spring model is used for mooring, which allows the stiffness of the mooring system to be freely specified for convenience. To directly transfer the rotor thrust to the mooring line as described in Section 2, the linear-spring mooring line is approximately colinear with the tension brace when the system is operating at equilibrium, assuming a steady rotor thrust of 1,500 kN (the IEA Wind 10-MW reference turbine has a steady-state thrust of 1,500 kN in near-rated wind and just under 600 kN at cutout wind speed [7]). A baseline spring stiffness of 100 kN/m is assumed for the mooring line.

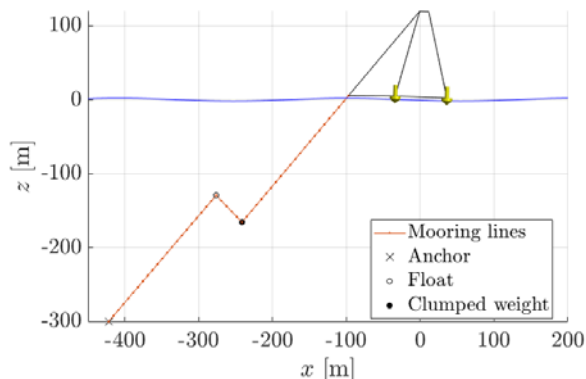


FIGURE 6: AN UNSTEADY LUMPED-MASS MOORING LINE MODEL FOR THE INITIALLY ENVISAGED CLUMP-EQUIPPED TAUT MOORING SYSTEM. (THE ROTOR IS NOT SHOWN.) FOR THE INITIAL DESIGN EXERCISE, A SIMPLE LINEAR-SPRING MODEL IS USED INSTEAD.

3.4 Aerodynamic modeling

The complete aeroelastic model of the IEA Wind 10-MW reference wind turbine is included in the OpenFAST model of the TOW FOWT concept. Furthermore, preliminary tuning of a Reference OpenSource Controller (ROSCO) [14] for the turbine has also been carried out. However, for the present initial design exercise on the sizing and arrangement of the platform based on its hydrodynamic performance, we opt to simplify aerodynamic effects by allowing the rotor to spin freely with the blades pitched to 90 deg (feathered) in quiescent air, thus minimizing aerodynamic loading. To capture the effects of steady wind thrust and limit mooring line slackening, a constant force of 1,500 kN is applied at the tower top normal to the rotor disk. Full aero-hydro-servo-elastic simulations with an operating rotor and

the tuned controller will be reported in the future. The AeroDyn module of OpenFAST with dynamic blade-element momentum theory for wake/inflow modeling and unsteady airfoil aerodynamics will be used to model the aerodynamic loads on the operating rotor.

4. RESULTS AND DISCUSSION

Initial parameters for the wave-following floating turbine design were selected via approximate analyses of simple loadings. The results indicated substantial enough benefits to justify more thorough investigations with OpenFAST.

We see ultimate loads as the most important to estimate (and possibly alter by revising the design) as they must be endured without failing. Fatigue accumulation might be less important, as an easily towed floating system designed for connecting and disconnecting could allow frequent shore-based inspection and repair. The initial OpenFAST simulation goal is therefore to evaluate peak accelerations and stresses from a suitable environmental contour.

For this preliminary analysis, we apply the typical standard-deviation-based procedure to estimate the expected 3-hour maximum response of the system. For any quantity Q , e.g., the hub acceleration in surge or the mooring tension, we use OpenFAST simulations with a series of regular waves of different frequencies or with white-noise waves to determine the frequency-dependent linear RAO. The standard deviation of Q in each sea state can be obtained using the RAO and the wave spectrum. The expected maximum value of Q for a 3-hour sea state is then estimated as 4 times the standard deviation [15].

The sea states considered are derived from the publicly available American Bureau of Shipping (ABS) 40-year North Atlantic environmental contour shown in Figure 7 [16]. The Joint North Sea Wave Project (JONSWAP) wave spectrum with a peak shape factor of 3.3 is assumed. The 40-year contour is chosen for its availability. Future load analyses will consider 1-year and 50-year return-period sea states as required by the International Electrotechnical Commission (IEC) 61400-3-1 design standard [17].

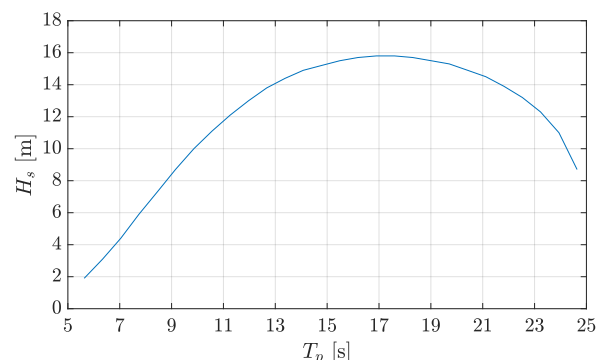


FIGURE 7. ABS 40-YEAR NORTH ATLANTIC REGION ENVIRONMENTAL CONTOUR WITH THE SIGNIFICANT WAVE HEIGHT, H_s , AS A FUNCTION OF WAVE PEAK PERIOD, T_p .

Some initial results are given for the original system (10-MW capacity, 70-m float spacing) of Figure 1. Figure 8 shows

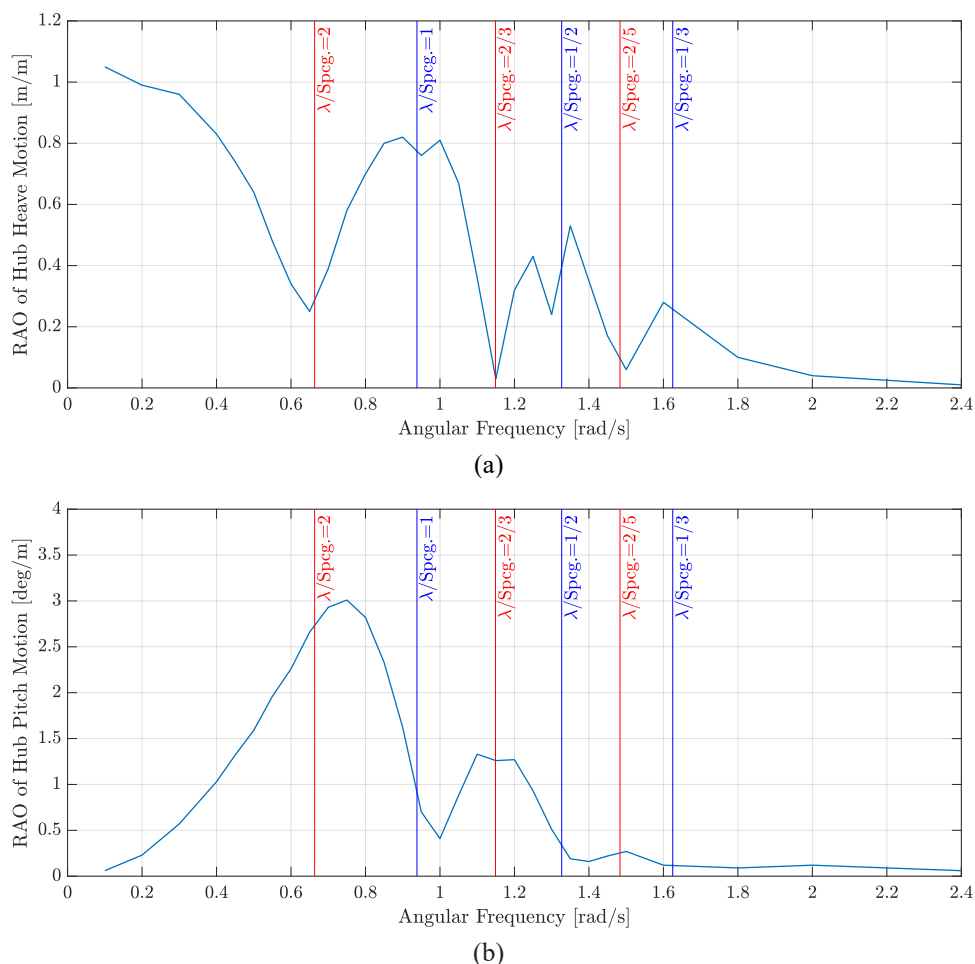


FIGURE 8: ESTIMATED HUB (a) HEAVE and (b) PITCH RESPONSE AMPLITUDE OPERATORS (RAO) WITH 70-m FLOAT SPACING (Spceg). THE RESULTS SHOWN ARE OBTAINED FROM A SERIES OF REGULAR-WAVE SIMULATIONS WITHOUT ANY MOORING AND TOWER-TOP LOAD. THE SYSTEM IS FULLY RIGID.

the frequency-dependent heave and pitch RAOs with no structural flexibility or mooring line. The results are derived from a series of regular-wave simulations with a constant wave height-to-wavelength ratio of 0.049, except for frequencies at or below 0.5 rad/s for which the wave height is limited to 11.5 m. Blue lines identify special wave frequencies that correspond to wavelengths, λ , placing all floats simultaneously at wave crests (or troughs). At these frequencies an ideal wave-following system will show a heave RAO of unity and a pitch RAO of zero. Red lines identify other frequencies, corresponding to wavelengths placing two floats at a crest and the other two in a trough. At these frequencies an ideal wave-following system will show a heave RAO of zero and a pitch RAO of $2\text{ m}/(70\text{-m float spacing})$ per meter of wave amplitude, or 1.64 deg/m . Deviation of the RAOs shown in Figure 8 from these expected values indicates departures from the ideal wave-following behavior, evident here in both the enlarged peak in pitch RAO at 0.75 rad/s (pitch resonance frequency) and the RAO attenuation at greater frequencies (shorter wavelengths) with both heave and pitch RAOs.

Peak rotor accelerations in the surge direction and in pitch about the sway axis are responsible for the maximum axle and tower bending stresses and impose the greatest demands on the bearings and generator. The 70-m-spacing results for the rotor's peak axial and pitch acceleration suggest that the former would create especially severe tower-top bending moments due to the legs (in side view) "intersecting" at a point eccentric from the rotor center of mass. To reduce this acceleration-induced leg bending, float spacing is increased and the structural design is revised. In Section 5, this design is illustrated, and some computed results are given.

5. UPDATES TO THE PLATFORM DESIGN

As discussed in Section 4, exploratory work with a rigid structure and 70-m float spacing suggests that a revised design might reduce the peak motions and stresses. This updated design is illustrated in Figure 9. The principal dimensions and the masses of the key components are summarized in Table 3 and Table 4. Mass is increased partly based on the input from turbine manufacturers.

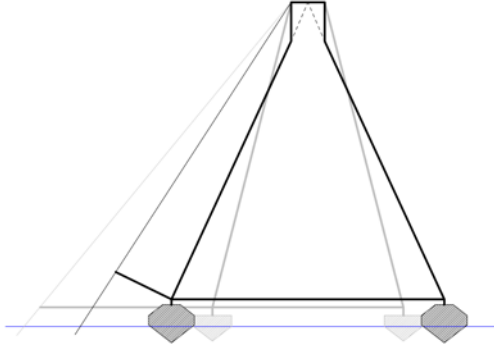


FIGURE 9: PROFILE OF THE IMPROVED DESIGN WITH WIDER FLOAT SPACING OVERLAYING THE ORIGINAL DESIGN DESCRIBED IN SECTION 2 IN LIGHT GRAY.

The improved design incorporates a wider (100-m) float spacing to reduce maximum pitch and the resulting hub acceleration in surge (since platform pitch is the main contributor to hub surge motion). The structural design is also improved with legs converging at the rotor center to eliminate bending induced by surge acceleration. The new design also incorporates a greater elevation angle of the mooring line to reduce pitch-induced displacement of the fairlead and consequent mooring line stretch.

TABLE 3: DIMENSIONS OF THE UPDATED DESIGN.

Dimension	Value	Unit
Float center-to-center distance	100	m
Hub height from still water level	119	m
Axle length between legs	12.3	m
Draft	5.97	m
Upwind distance from rotor to fairlead	70.4	m
Maximum float diameter	16.8	m
Float cone height	6.57	m

TABLE 4: UPDATED MASSES OF KEY COMPONENTS.

Component	Mass	Unit
Mass of floats	410	Metric ton
Mass of tower legs	368	Metric ton
Rotor mass (hub, blades, and generator rotor)	357	Metric ton
Axle assembly mass (axle tube, generator stator, generator add-on)	226	Metric ton
Structural bracing and mooring standoff	139	Metric ton
Total mass	1,500	Metric ton

To investigate the impact of structural flexibility, the OpenFAST results obtained with a fully flexibly system are compared to those obtained with rigid turbine blades and/or a rigid platform. The blades can be rendered rigid in OpenFAST by disabling all blade-bending DoF in ElastoDyn. The platform can be made rigid by setting the number of Craig-Bampton modes retained to zero and disabling the static improvement method (see Section 3.1). Figure 10 shows the heave and pitch RAOs—now calculated via white-noise wave excitation with 2-m significant wave height [18]—of the updated design with 100-m float spacing estimated for a linear-spring mooring line of stiffness 100 kN/m and 1,500 kN tower-top load. The effects of structural flexibility are investigated by making both platform and blades rigid (RR), then with a flexible platform plus rigid

turbine blades (FR), and lastly a flexible platform with flexible blades (FF). In Figure 10a, the fully rigid RR system has greater heave-response peaks above 1.3 rad/s. On the other hand, blade flexibility has very limited impact on heave response; the results obtained with a flexible platform with and without blade flexibility (FR and FF) are nearly identical for all wave frequencies.

Structural flexibility has a greater impact on hub pitch response as shown in Figure 10b. The RR system displays a prominent peak in pitch response near 1.25 rad/s that is suppressed by a flexible platform (see FR and FF with nearly identical responses for frequencies below 1.8 rad/s). However, above approximately 1.9 rad/s, the hub pitch response is least for the RR system. Full flexibility (FF) produces a peak in hub pitch response at 2.2 rad/s. Notably, the highest pitch-RAO peak is greatly reduced with the 100-m float spacing compared to 70-m float spacing in Figure 8b, though not quite to the ideal value of 1.15 deg/m expected from perfect wave-following behavior with 100-m float spacing.

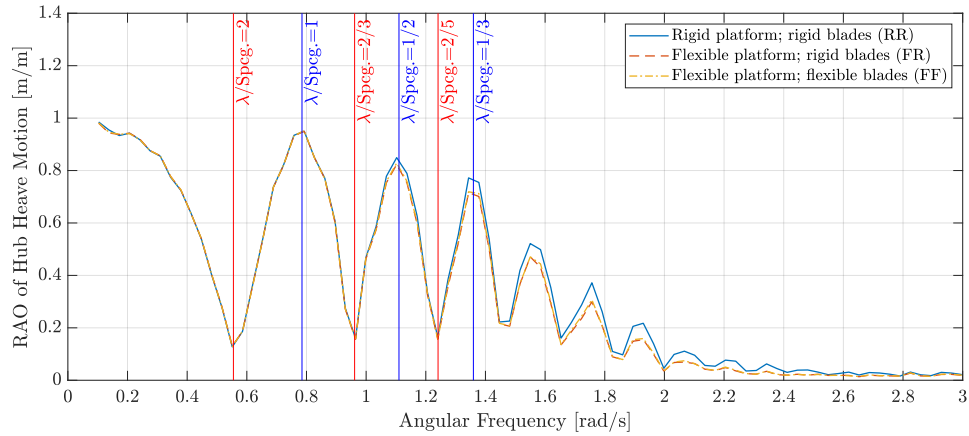
Figure 11 compares the root-mean-square (RMS) values of hub axial/surge acceleration estimated based on the ABS 40-year environmental contour (Figure 7), first with the original 70-m-spacing rigid unmoored design, then with the proposed new 100-m-spacing design. Compared to the original design, the 100-m RR results indicate a 44% reduction in the most severe acceleration. However, the most severe acceleration increases by 16% when platform flexibility is considered (FR and FF). Blade flexibility shows negligible impact on RMS hub axial acceleration.

The reduced acceleration achieved with 100-m float spacing is of central importance. It suggests that the worst hub axial acceleration on the 40-year contour, estimated as 4 times the RMS value, might be limited to approximately 1g. The key question to be answered is whether the costs of accommodating this acceleration outweigh the anticipated savings from the shallow-draft, lightweight platform design.

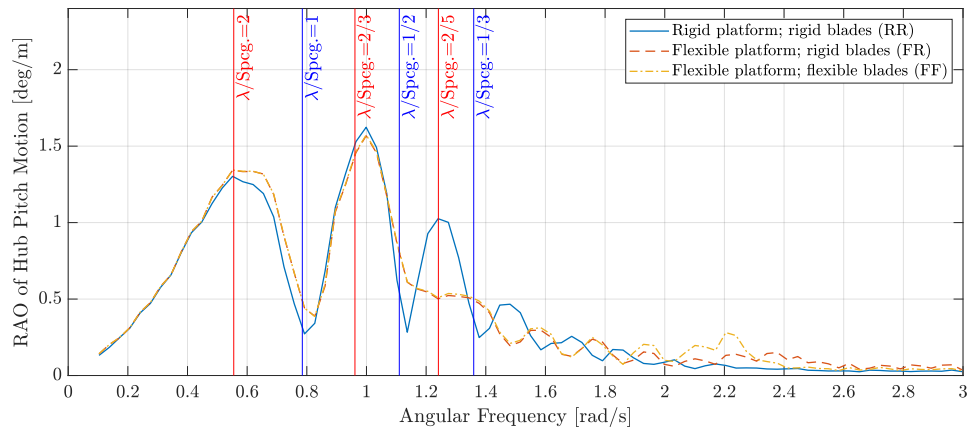
6. CONCLUSIONS

An OpenFAST model is developed for the TOW wave-following FOWT platform concept. Compared to prior analyses based on simplifying assumptions, this coupled model allows the design to be evaluated through more realistic simulations, incorporating the effects of platform flexibility, mooring load, rotor aero-elastics, controls, etc., although only an approximated tower-top load representing the rotor thrust is applied in this work.

Simulations with the original platform design without structural flexibility, mooring, and tower-top load reveal some issues, chiefly the large platform pitch response that deviates substantially from the ideal wave-following behavior envisaged for the TOW platform concept. The large pitch response can result in excessive acceleration at the rotor hub and, by extension, high blade and bearing loads and leg bending moments.



(a)



(b)

FIGURE 10: HUB (a) HEAVE AND (b) PITCH RESPONSE AMPLITUDE OPERATORS (RAO) WITH 100-m FLOAT SPACING (spcg), LINEAR-SPRING MOORING, AND TOWER-TOP LOAD ESTIMATED FROM SIMULATIONS WITH WHITE-NOISE WAVES. THE RESULTS ARE COMPUTED FROM 1 HOUR OF TIME HISTORY DIVIDED INTO 20 PARTS FOR ENSEMBLE AVERAGING.

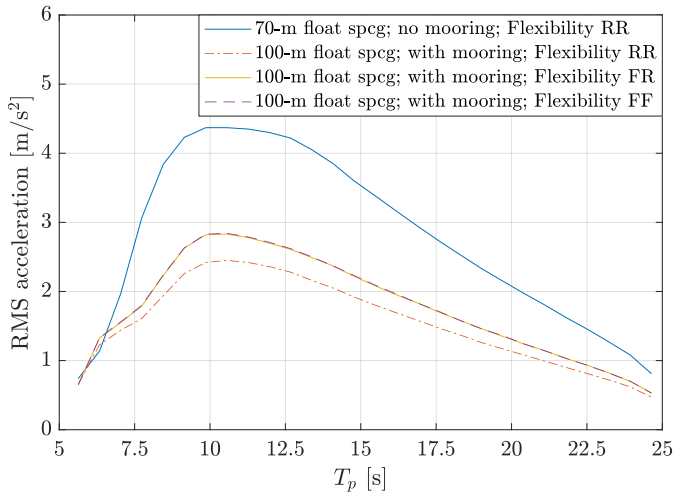


FIGURE 11: ROOT-MEAN-SQUARE (RMS) AXIAL HUB ACCELERATION WITH DIFFERENT FLOAT SPACINGS (spcg) IN RESPONSE TO THE ENVIRONMENTAL CONTOUR OF FIGURE 7.

To address the issues identified, an updated design is developed and evaluated through OpenFAST simulations. The new design with increased float spacing has significantly reduced pitch response that is much closer to the ideal wave-following behavior; however, platform structural flexibility tends to increase the pitch response and hub acceleration. With the updated design, the extreme hub surge acceleration estimated using the 40-year return-period North Atlantic environmental contour is just over $1g$ with structural flexibility.

Compared to more traditional wave-transparent designs, the wave-following platform concept is expected to have increased tower-top motion. The present analysis through OpenFAST simulations succeeds in showing that the tower-top acceleration can be realistically limited to approximately $1g$ with this wave-following concept. Therefore, whether such a design can be economically competitive depends on whether the cost reduction derived from the lightweight and shallow-draft platform outweighs the increased cost of building wind turbines that can withstand this level of hub acceleration. This question remains to be answered.

7. FUTURE WORK

A follow-up study will use more realistic wave and wind loading to solidify structural requirements. The design of the mooring system will also need to be addressed. A low mooring stiffness is desirable to minimize disturbances to the platform's wave-following behavior and to avoid slackening events that cause snap loads. Since achieving low stiffness with adequate strength is a challenge with short line lengths (i.e., in shallow water), a linear-spring representation of the mooring system with 100 kN/m stiffness was adopted initially. In the future, the mooring stiffness will be increased up to the point where platform motion is affected to identify the highest allowable mooring stiffness that minimizes the design challenge.

With the overall platform and mooring configuration solidified, global load analyses of the TOW FOWT concept will be conducted through coupled aero-hydro-servo-elastic simulations of the IEC design load cases. The fidelity of the OpenFAST hydrodynamic model will be further enhanced by switching to a nonlinear and exact hydrostatic load calculation and/or with hydrodynamic coupling among the floats and second-order wave excitation. An unsteady lumped-mass model of the mooring system can also be used, along with further fine-tuning of the turbine controller.

In addition, plans are being developed to enhance AeroDyn to support more complex tower arrangements with load coupling to the SubDyn substructure module of OpenFAST. This will enable aeroelastic analysis of the multi-legged tower design. Support for large system yaw rotation will also be added to OpenFAST to simulate the transient response to yaw misalignment and thereby evaluate the design's weathervaning performance. Solutions such as individual blade pitch control will be explored to enhance the control of platform yaw motion.

Finally, the slamming pressure on the bottom of the shallow-draft floats needs to be investigated using known correlations with water-penetration velocity. This is especially important for conditions involving quartering seas, where one of the floats could lift out of the water.

ACKNOWLEDGEMENTS

This work was authored in part by the National Renewable Energy Laboratory, operated by Alliance for Sustainable Energy, LLC, for the U.S. Department of Energy (DOE) under Contract No. DE-AC36-08GO28308. Funding provided by the National Science Foundation STTR Phase I program under award number 2136763, a project started in 2022 titled "Validation of a Floating Wind Turbine Platform Optimized for Low Cost and Extensive Deployment." The views expressed in the article do not necessarily represent the views of the DOE or the U.S. Government. The U.S. Government retains and the publisher, by accepting the article for publication, acknowledges that the U.S. Government retains a nonexclusive, paid-up, irrevocable, worldwide license to publish or reproduce the published form of this work, or allow others to do so, for U.S. Government purposes.

REFERENCES

- [1] Stehly, T. and Duffy, P., (2021), "2020 Cost of Wind Energy Review," National Renewable Energy Laboratory, Golden, CO, USA.
- [2] Papadopoulos, J.M., Qiao, C. and Myers, A.T., (2021), "Concept for a wind-yawing shallow-draft floating turbine," in *Proceedings of the ASME 2021 3rd International Offshore Wind Technical Conference*, Virtual, Online, p. V001T01A013.
- [3] Connolly, A., Guyot, M., Le Boulluec, M., Héry, L. and O'Connor, A., (2018), "Fully coupled aero-hydro-structural simulation of new floating wind turbine concept," in *Proceedings of the ASME 2018 1st International Offshore Wind Technical Conference*, San Francisco, CA, USA, p. V001T01A027.
- [4] Guyot, M., De Mourgues, C., Le Bihan, G., Parenthoine, P., Temploi, J., Connolly, A. and Le Boulluec, M., (2019), "Experimental offshore floating wind turbine prototype and numerical analysis during harsh and production events," in *Proceedings of the ASME 2019 2nd International Offshore Wind Technical Conference*, St. Julian's, Malta, p. V001T02A004.
- [5] Riyanto, R.D., Papadopoulos, J.M. and Myers, A.T., (2022), "Numerical investigation of wave following mechanism of shallow draft floating wind turbine," in *Proceedings of the ASME 2022 4th International Offshore Wind Technical Conference*, Boston, MA, USA, p. V001T01A017.
- [6] Jonkman, J.M., (2013), "The new modularization framework for the FAST Wind Turbine CAE Tool," in *Proceedings of the 51st AIAA Aerospace Sciences Meeting including the New Horizons Forum and Aerospace Exposition*, Grapevine, TX, USA.
- [7] Bortolotti, P., Tarrés, H.C., Dykes, K.L., Merz, K., Sethuraman, L., Verelst, D. and Zahle, F., (2019), "IEA Wind TCP Task 37: Systems engineering in wind energy - WP2.1 reference wind turbines," National Renewable Energy Laboratory, Golden, CO, USA.
- [8] Jonkman, J., Branlard, E., Hall, M., Hayman, G., Platt, A. and Robertson, A., (2020), "Implementation of substructure flexibility and member-level load capabilities for floating offshore wind turbines in OpenFAST," National Renewable Energy Laboratory, Golden, CO, USA.
- [9] Wang, L., Jonkman, J., Hayman, G., Platt, A., Jonkman, B. and Robertson, A., (2023), "Recent hydrodynamic modeling enhancements in OpenFAST," in *Proceedings of the ASME 2022 4th International Offshore Wind Technical Conference*, Boston, MA, USA, p. V001T01A004.
- [10] Jonkman, J.M., Damiani, R.R., Branlard, E.S.P., Hall, M. and Robertson, A.N., (2019), "Substructure flexibility and member-level load capabilities for floating offshore wind turbines in OpenFAST," in *Proceedings of the ASME 2019*

- 2nd International Offshore Wind Technical Conference*, St. Julian's, Malta, p. V001T01A004.
- [11] Damiani, R., Jonkman, J. and Hayman, G., (2015), "SubDyn user's guide and theory manual," National Renewable Energy Laboratory, Golden, CO, USA.
- [12] Krathe, V.L., Jonkman, J. and Bachynski-Polić, E.E., (2023), "Implementation of drivetrain structural flexibility in OpenFAST," presentation in *EERA DeepWind 2023*, Trondheim, Norway.
- [13] Cummins, W.E., (1962), "The impulse response function and ship motion," David Taylor Model Basin, Washington, D.C., USA.
- [14] Abbas, N.J., Zalkind, D.S., Pao, L. and Wright, A., (2022), "A reference open-source controller for fixed and floating offshore wind turbines," *Wind Energ. Sci.*, Vol. 7, pp. 53–73.
- [15] Chen, C.-Y. and Mills, T., (2010), "On Weibull extreme response of offshore structures," in *Proceedings of the ASME 2010 29th International Conference on Ocean, Offshore and Arctic Engineering*, Shanghai, China, pp. 295-302.
- [16] American Bureau of Shipping, (2021), "Guide for slamming loads and strength assessment for vessels," American Bureau of Shipping, Spring, TX, USA.
- [17] International Electrotechnical Commission, (2018), "IEC 61400-3-1 Wind energy generation systems – Part 3-1: Design requirements for fixed offshore wind turbines," International Electrotechnical Commission, Geneva, Switzerland.
- [18] Ramachandran, G.K.V., Robertson, A., Jonkman, J.M. and Masciola, M.D., (2013), "Investigation of response amplitude operators for floating offshore wind turbines," in *Proceedings of the 23rd International Offshore and Polar Engineering Conference*, Anchorage, Alaska, USA.